이학석사 학위논문

Expression Profiling of Human Thyroid Cell Line Stably Expressing $BRAF^{V600E}$ Mutation

$BRAF^{V600E}$ 돌연변이를 과발현하는 인간 갑상선 세포주의 발현 양상 연구

2016년 8월

서울대학교 대학원

협동과정 종양생물학 전공

김 병 애

A thesis of the Master's degree

BRAF ^{V600E} 돌연변이를 과발현하는 인간 갑상선 세포주의 발현 양상 연구

Expression Profiling of Human Thyroid Cell Line Stably Expressing BRAF^{V600E} Mutation

August 2016

Interdisciplinary Program in Tumor Biology

Seoul National University Graduate School

Byoung-Ae Kim

Abstract

Introduction: BRAF V600E mutation is the most common somatic mutation in papillary thyroid carcinoma (PTC) and act as an initiator of cancer development. Gene expression change caused by BRAFV600E mutation might play an important role for thyroid cancer development.

Methods: To study the genomic alteration caused by BRAF V600E mutation, we made human thyroid cell lines which harbor wild type BRAF gene (Nthy/WT) and V600E mutant type BRAF gene (Nthy/V600E). Successful transduction of BRAF gene was evaluated by flow cytometry and Sanger sequencing. Phosphorylation of ERK was anlayzed by flow cytometry and western blot. Functional changes of the cells according to BRAFV600E mutation were observed by soft agar and invasion assay. Microarray analysis was performed to find differentially expressed genes between BRAF wild and BRAFV600E cells.

Results: BRAF gene was successfully transfected into Nthy-ori cell, confirmed by Sanger sequencing in both Nthy/WT and Nthy/V600E. Flow cytometry and Western blot showed stable transfection amount of BRAF gene. In functional experiments, Nthy/V600E cells have increased phophorylated ERK levels, higher anchorage-independent grow rate, and enhanced Matrigel invasion in vitro. Microarray analysis reveals that 2441 genes were up-regulated in Nthy/V600E cells; top 3 up-regulated genes were IL1B, ANO1, and SERPINE2. Up-regulated genes are associated with cell adhesion, migration, motility, ERK and MAPK cascade in gene ontology. Cancer related pathways also enriched in pathway analysis.

Conclusions: Our Nthy/WT and Nthy/V600E cell lines, with its correlation with human BRAFV600E PTCs, may be used as a source for basic experiments to further research for molecular characteristics of thyroid cancer.

Keywords: Thyroid, Nthy-ori 3-1 cell, $BRAF^{V600E}$, transduction, microarray

Student Number: 2014-25079

Contents

List of Figures

List of Tables

Introduction

BRAFV600E mutation is well known driver mutation with a single nucleotide change of thymine into adenine at 1799th site of BRAF gene. This mutation results in a valine-to-glutamic acid substitution at amino acid site 600 (c1799T>A, pV600E) and leads to carcinogenesis by activates BRAF kinase cascade (1). BRAFV600E mutations accounts for 95% of BRAF gene alterations and it the most common genetic variation in papillary thyroid carcinomas (PTC) (2). Prevalence of BRAFV600E mutation is generally known as 29-83% worldwide (3).

Previous studies have reported that the BRAFV600E mutation is correlated with advanced disease status such as extrathyroidal extension or lymph node metastasis but it is not clearly linked with overall survival. For this reason, secondary gene expression changes caused by BRAF V600E mutation are thought to be an important roles for thyroid cancer progression (4-6).

In vitro study using thyroid cell lines, ARO, KAT10 and NPA mainly used as BRAF V600E mutation group (7). There is a limit as BRAF V600E mutation group in that the BRAF V600E mutation is not the only variable because the cells derived from human thyroid cancer. PCCL3 and FRTL-5 is normal thyroid cell line, but the cells derived from rodent. It seems to need a study to compare the expression of BRAF wild type and BRAF mutant type in normal human thyroid cell lines.

Nthy-ori 3-1 is an immortal thyroid follicular epithelial cell line derived from normal thyroid tissue of an human that has been transfected with a

plasmid encoding for the SV40 large T gene. Nthy-ori 3-1 is highly suitable for transfection experiments and is useful for in vitro studies of the human thyroid (8).

The Nthy-ori 3-1(Nthy) cell line is a valuable tool for molecular analysis of thyroid carcinomas because it is the only human thyrocyte cell line with continuous growth in vitro. We successfully developed Nthy/BRAF cells using lentivirus system, not only wild type but also BRAF V600E mutant type. Using this Nthy/BRAF cell, we conducted functional and genomic experiments to explore the biologic and genomic alteration in normal thyroid cells initiated by BRAFV600E mutation.

Materials and Methods

1. Induction of BRAF gene into Nthy cell by Lentivirus transduction

Full coding sequences of BRAF wild type and BRAF V600E were amplified by PCR from TPC1 and 8505c cells. PCR amplification products were sub-cloned into the pCDH-MCS-T2A-copGFP-MCSV lentiviral vector (System Biosciences, Mountain View, CA, USA) and packaged by co-transfection with psPAX2 and pMD2.G plasmids (Addgene 12260 and 12259) with Lipofectamine 2000 (Invitrogen, Carlsbad, CA,USA) in HEK293FT (Invitrogen, Carlsbad, CA,USA) cells. Virus was harvested and concentrated by ultracentrifugation 48 hours later. Titers were determined by flow cytometry as percentage of Green Fluorescent Protein (GFP) positive cells. For stable cell line generation, Nthy-ori 3-1 cells were treated with different titers of lentivirus for 24 hours and examined for GFP expression after 3 days. Titers with 95%+ GFP positive cells were chosen for further culture. When necessary, cells with similar GFP expression were sorted using FACSAria (BD biosciences, San Jose, CA, US).

2. Verification of BRAF Gene Transduction

1) Cell Morphology Inspection and DNA Sequencing

Transfected cells were observeded with an inverted microscope. Each transfected cells were cultured in 60 mm dishes. Cultured cells were detached

using a cell scraper. Genomic DNA was extracted using QIAamp DNA Kits (Qiagen, Hilden, Germany), according to the manufacture's recommendations. DNA was quantified using a Nanodrop ND-1000 spectrophotometer and used as template for PCR amplification. PCR was performed using GeneAmp® PCR System 9700 (Applied Biosystems; Life Technologies, Carlsbad, CA, USA): initial denaturation at 95°C for 1min followed by 35 cycles of denaturation at 95°C for 15 seconds, annealing at 58°C for 15 seconds, extension at 72°C for 15 seconds. PCR primer and DNA sequencing services were provided by Cosmo Genetech (Cosmo Genetech, Seoul, Korea). The primer sequences used in this study are as follow:

BRAF exon 15: F 5'-TGAAGACCTCACAGTAAAAATAGGTG-3',

BRAF exon 15: R 5'- TCCACAAAATGGATCCAGACA-3'.

2) Flow cytometry

Nthy cells infected by empty, BRAF wild, BRAF V600E lentiviruses were fixed with FCM fixation buffer (Santa cruz biotechnology, Santa Cruz, CA, USA) on ice for 15 minutes. Fixed samples were washed in PBS and permeabilized on ice for 10 minutes in FCM Permeabilization buffer (Santa cruz biotechnology, Santa Cruz, CA, USA). Samples were washed and re-suspended, and incubated with phycoerythrin (PE) conjugated Phospho-p44/42 MAPK (Cell Signaling Technology; Beverly, MA, USA) for 1 hour. The labeled cells were detected by the BD FACS Diva 8.0 Systems (Becton Dickinson, San Jose, CA, USA) according to the manufacturer's protocols. Gating was implemented on the basis of negative control staining profiles.

3) Western blotting

Cells were cultured in 100 mm dishes with RPMI1640 with 10% FBS and penicillin-streptomycin . When cells were 80% confluent, the media was changed with RPMI1640 with or without FBS and further incubated for 24 hours. Cells were washed twice with phosphate buffered saline (PBS), detached from the culture plate using a cell scraper. Cells were lysed on ice for 15 minutes with a radio-immuno-precipitation assay (RIPA) buffer (Thermo Scientific, IL, USA) which contains 1% proteinase inhibitors. The samples were loaded onto a 10% SDS-polyacrylamide gel and subjected to electrophoresis on ice. The resolved protein were transferred on to polyvinylidene fluoride (PVDF) membrane for 1 hour and were blocked for 1 hour at room temperature with 5% skim milk. The membrane were incubated overnight at 4°C with the primary antibodies. Alpha Tubulin Antibody (1:1000 diluted) was obtained from Santa Cruz Biotechnology, ERk1/2 antibody (1:1000 diluted) and phospho-ERK1/2 antibody (1:1000 diluted) were was obtained from Cell Signaling Technology.

3. Biologic Evaluation of Nthy/BRAF Cells

1) Soft agar assay

Nthy cells infected with empty, BRAF wild, BRAFV600E lentiviruses were seeded at 3,000 cells per well in 24-well plates in a top layer of 0.4% agarose (Cell biolabs) on a base layer of 0.6% agarose. Culture medium containing DMSO or BRAFV600E kinase inhibitors (PLX-4032; Bio vision) were added to each well and cultured at 37 °C in the presence of 5% CO2 for 7 days. We

counted the number of colonies using microscope. The number of colonies containing more than 25 cells was counted under a microscope to determine the rate of colony formation.

2) Invasion assay

Invasion assay was performed using the xCELLigence DP Real Time Cell Anlayzer and CIM-16 plates with 8 μm pore membranes. The bottom electrodes of CIM-16 plates were coated with 0.2% gelatin and incubated in a laminar air flow chamber for 30 minutes. The upper chambers of CIM-16 plates were coated with 20 μl of 0.5 mg/ml Growth Factor Reduced Matrigel (BD Bioscience, Bedford, MA, USA) prepared in FBS-free RPMI media. Matrigel was allowed to equilibrate for 2 hours at 37 °C in a 5 % CO2. RPMI media with 10% FBS was added to the bottom chambers. Vector control cells (Nthy/Vector), BRAF wild type cells (Nthy/WT), or BRAFV600E cells (Nthy/V600E) were added on top compartments, 0.8 x105 cells per well. The impedance data, reported as Cell Index and is proportional to the area which migrated/invaded cells cover the bottom electrodes, were collected every 15 minutes. The percentage of invasion was calculated by the ratio of the invaded cells to the migrated cells (9).

3) Gene expression microarray

Total RNA was extracted using easy-spin (DNA free) Total RNA Extraction Kit (iNtRON Biotechnology, Seoul, Korea) and quantified using a Nanodrop ND-1000 spectrophotometer (NanoDrop, Wilmington, DE, USA). Microarray services were provided by Macrogen (Macrogen Inc., Seoul, Korea) using the Illumina HumanHT-12 v4 Expression BeadChip (Illumina, Inc., San Diego, CA). Total RNA was amplified and purified using TargetAmp-Nano Labeling

Kit for Illumina Expression BeadChip (EPICENTRE, Madison, USA) to yield biotinylated cRNA according to the manufacturer's instructions. Briefly, 500 ng of total RNA was reverse-transcribed to cDNA using a T7 oligo (dT) primer. Second-strand cDNA was synthesized, in vitro transcribed, and labeled with biotin-NTP. After purification, the cRNA was quantified using the ND-1000 Spectrophotometer (NanoDrop, Wilmington, USA). 750 ng of labeled cRNA samples were hybridized to each Human HT-12 v4.0 Expression Beadchip for 17 hours at 58°C, according to the manufacturer's instructions (Illumina, Inc., San Diego, USA). Detection of array signal was carried out using Amersham fluorolink streptavidin-Cy3 (GE Healthcare Bio-Sciences, Little Chalfont, UK) following the bead array manual. Arrays were scanned with an Illumina bead array Reader confocal scanner according to the manufacturer's instructions.

We performed microarray experiment with two group according to BRAFV600E mutation status. WD 10F group was two wild type BRAF cells treated with growth factor and MT 10F group was two mutant type BRAF cells with treated with growth factor. Raw data which derived from the Illumina Genome Studio version 2011.1 and Gene Expression Module version 1.9.0 were analyzed by "lumi R package" version 1.1.0. Packages "annotate" and "illuminaHumanv4.db" were used for microarray chip probe annotation, served by bioconductor (http://www.bioconductor.org). To find differentially expressed genes (DEGs), linear discriminant analysis was applied using the "limma" package (10). P-value under 0.05 after BH correction was considered as statistical significance. Log fold change value 2 was considered as cutoff for significant DEG. DEGs underwent pathway analysis using the Database

for Annotation, Visualization and Integrated Discovery (DAVID) v6.7(11). “GO stat” package was used for functional and pathway analysis(12). Benjamini-Hochberg (BH) method were used for correcting false positive rate from multiple comparison. All statistical analysis were performed by R version 3.2 (13).

Results

Effect of BRAF gene transduction into Nthy cell

Nthy cells were stably transfected with empty vectors, BRAF wild and BRAFV600E; named as Nthy/Vector, Nthy/WT and Nthy/V600E, respevtively. Cell morphology of Nthy/Vector and Nthy/WT cells were in similar shape with the parental Nthy-ori 3-1. However, Nthy/V600E cells have a spindle transformed shape as shown in figure 1A.

BRAF gene sequences of these cells were confirmed by Sanger sequencing. As shown on figure 1B, BRAF exon 15 sequences flanking 1799th nucleotide of Nthy/Vector and Nthy/WT cells were normal. Nthy/V600E cells, however, had a mutation on 1799th site, T>A. This result shows that the BRAFV600E recombinant plasmid was successfully constructed and expressed in Nthy-ori 3-1 cell, at a level surpassing the original wild type BRAF.

In the flow cytometry results (Figure 2A), the marker protein GFP showed similar peak fluorescence intensity among the Nthy/Vector, Nthy/WT and Nthy/V600E, indicating similar BRAF protein expression level in the cells. The intensity of p-ERK was increased in Nthy/V600E group compared to that of Nthy/Vector or Nthy/WT group (Figure 2A). Increased expression of p-ERK was also confirmed by western blot (Figure 2B).

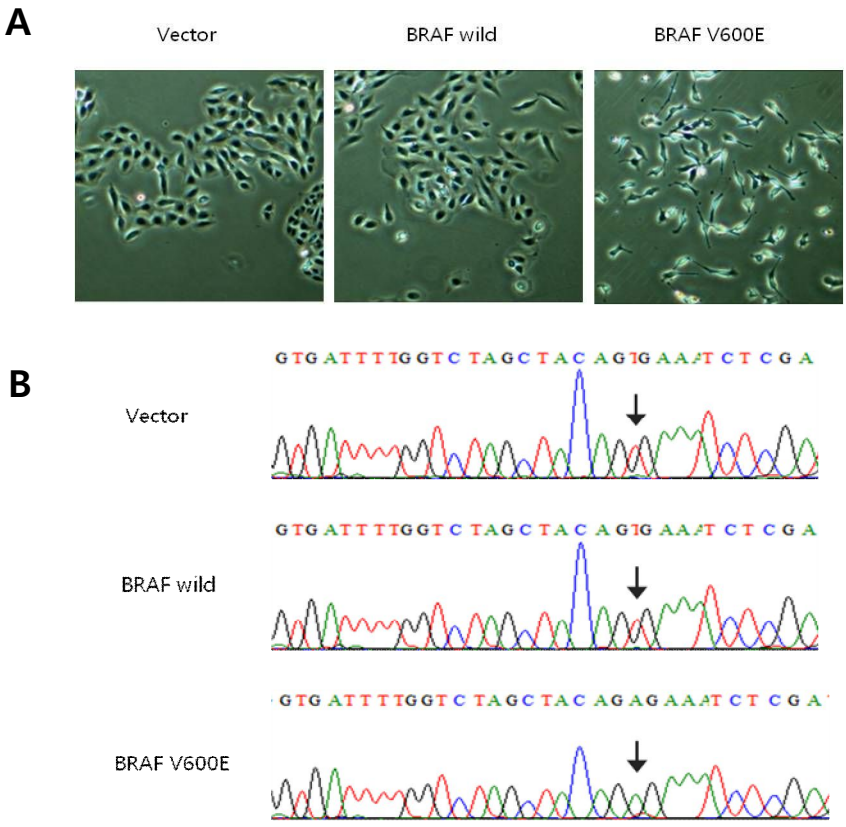

Figure 1. Cellular morphology and BRAF sequences of Nthy/Vector, Nthy/WT and Nthy/V600E cells.

A, cells were cultured in RPMI medium with 10% FBS and photographed using inverted microscope (40×). B, BRAF exon 15 sequences of Nthy/Vector, Nthy/WT and Nthy/V600E cells.

A

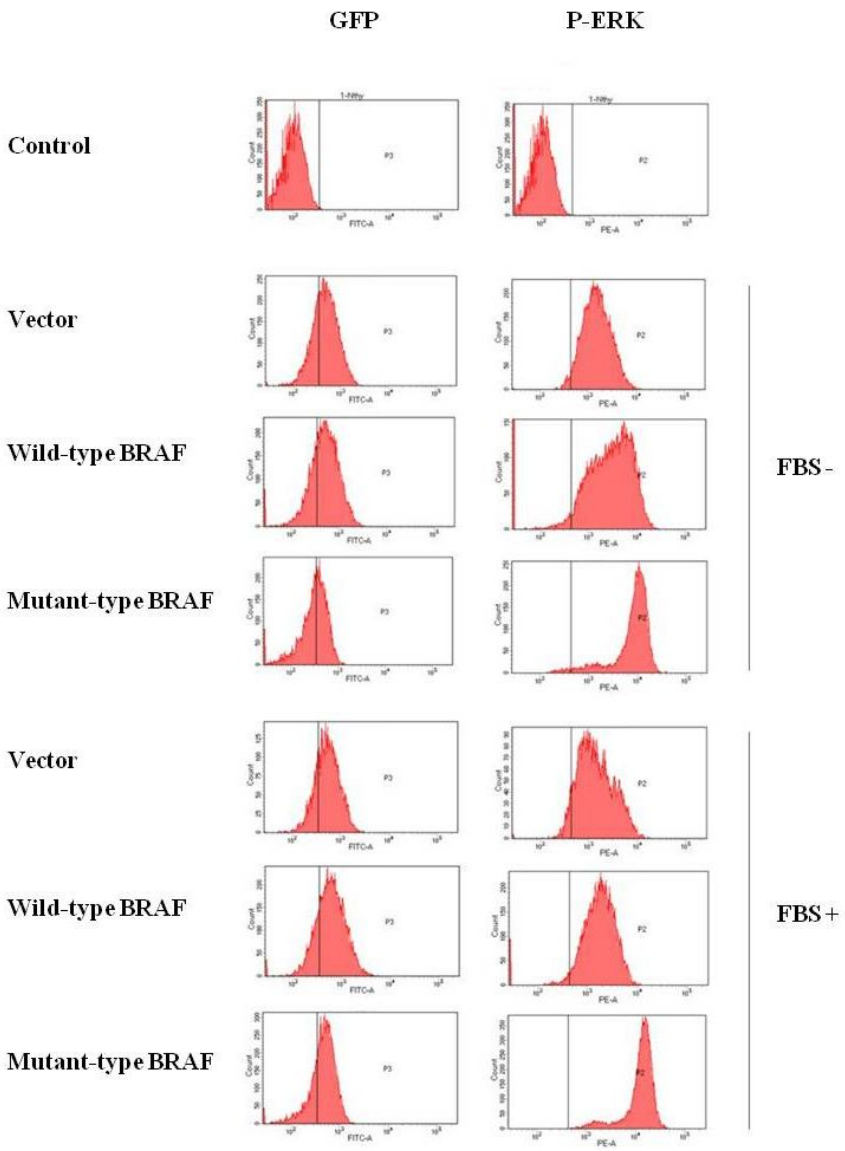
GFP
P-ERK
Control
Vector
Wild-type BRAF
Mutant-type BRAF
Vector
Wild-type BRAF
Mutant-type BRAF
FBS -
FBS +
FITC-A
PE-A

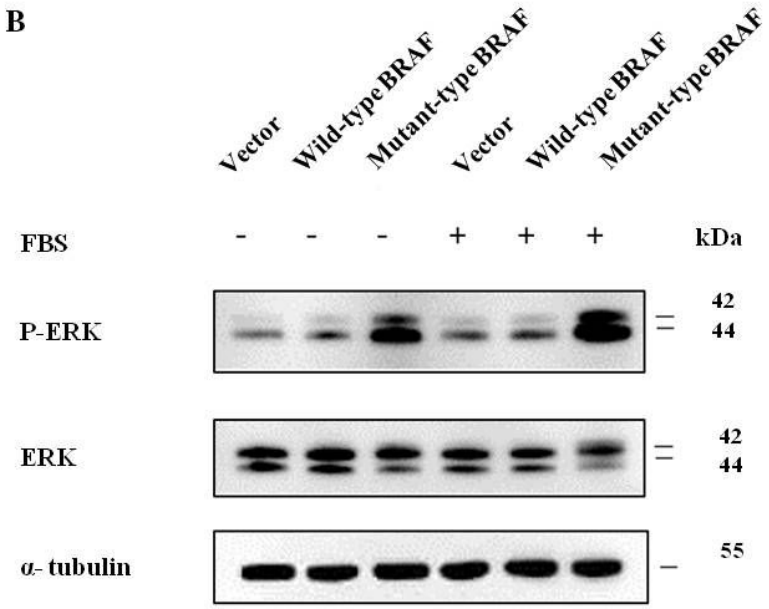

Figure 2. Phosphorylation level of ERK in Nthy/Vector, Nthy/WT and Nthy/V600E cells.

A, Phosphorylation level of ERK by flow cytometry. Cells were cultured RPMI medium with or without 10% FBS for 24 hours prior to detach. Control is parental Nthy-ori 3.1 cells cultured RPMI medium with 10% FBS. B, Protein expression levels of phosphorylated ERK and ERK using Western blot. Cells were cultured RPMI medium with or without 10% FBS during 24 hours prior to analysis. α-tubulin was served as a control.

Increased anchorage-independent growth and invasion ability in Nthy/V600E cells

Soft agar assay results for estimating anchorage independent growth patterns of cells are illustrated in figure 3. The number of colonies observed was higher in Nthy/V600E compared with Nthy/Vector or Nthy/WT. Treatment of different dose of the PLX4032, a potent kinase inhibitor of BRAFV600E, inhibited colony growth but the growth reduction was not prominent in Nthy/Vector and Nthy/WT cells. Cell colony formation rate showed a dose-related growth decrement in Nthy/V600E. Invasion/migration ratio in cell invasion assay was increased only in the Nthy/V600E (Figure 4). From these results, we suggest that Nthy/V600E cells have increased anchorage independent growth pattern and stronger invasive potential.

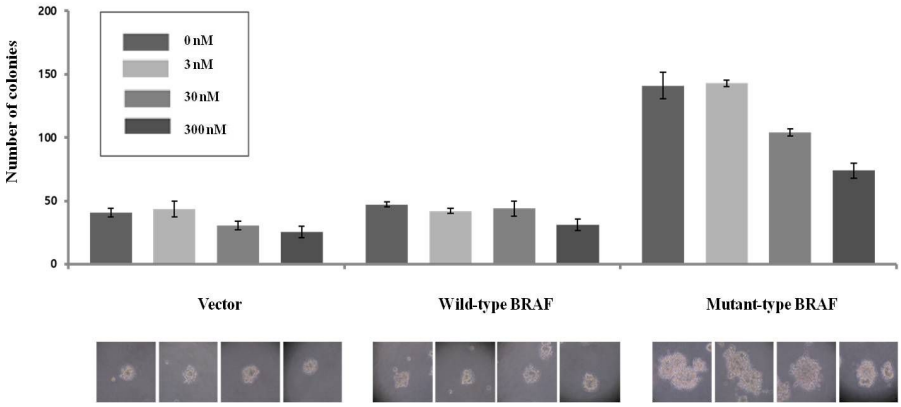

Figure 3. Cell colony formation of Nthy/Vector, Nthy/WT and Nthy/V600E cells.

Cells were grown on a 3-dimensional agar gel and treated with different dose of the PLX4032, which is a potent kinase inhibitor of BRAFV600E. Representative cell colony images are shown.

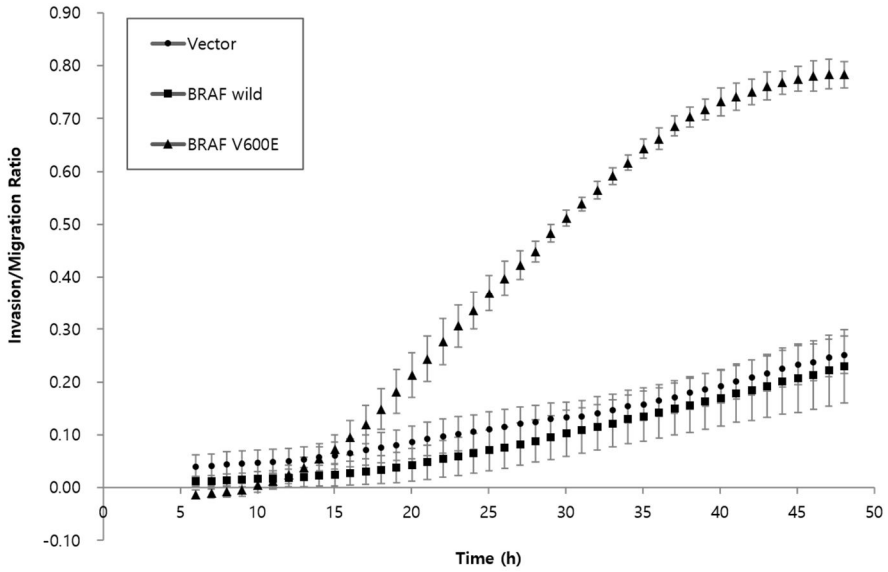

Figure 4. Invasion/Migration ratio of Nthy/Vector, Nthy/WT and Nthy/V600E cells.

Covered area of bottom electrodes, which is proportional to the invaded (Matrigel-coated) or migrated (not coated) cell numbers, were measured using Real Time Cell Analyzer. The percentage of invasion was calculated by the ratio of the invaded cells to the migrated cells.

Gene expression microarray result

A total of 2441 genes were expressed higher in Nthy/V600E cells compared with Nthy/WT cells (Figure 5). Twenty-two genes were satisfied with the cutoff of significantly up-regulated DEGs (BH p-value < 0.05 and log fold change > 2) in Nthy/V600E cells (Table 1). Top three overexpressed genes were IL1B, ANO1, SERPINE2, respectively.

In the gene ontology (GO) analysis, 210 gene ontologies were enriched in the Nthy/V600E cells (Table 2). Enriched GO terms in Nthy/V600E cells which were concordant with our functional analysis were as follows: (1) morphology chance into spindle shape - “cell morphogenesis”, (2) increased cell growth in softagar - “cell differentiation”, “cell growth”, “cell motility”, “cell migration” (3) enhanced invasion ability - “cell motility”, “cell adhesion”, (4) overexpression of p-ERK - “ERK1 and ERK 2 cascade”,“MAPK cascade”.

Pathway analysis, derived from DAVID program using DEGs as input, are listed in table 2. Pathways in cancer, other cancer related pathways such as lung or colorectal cancer, cell cycle and p53 signaling pathway were enriched in Nthy/V600E cells.

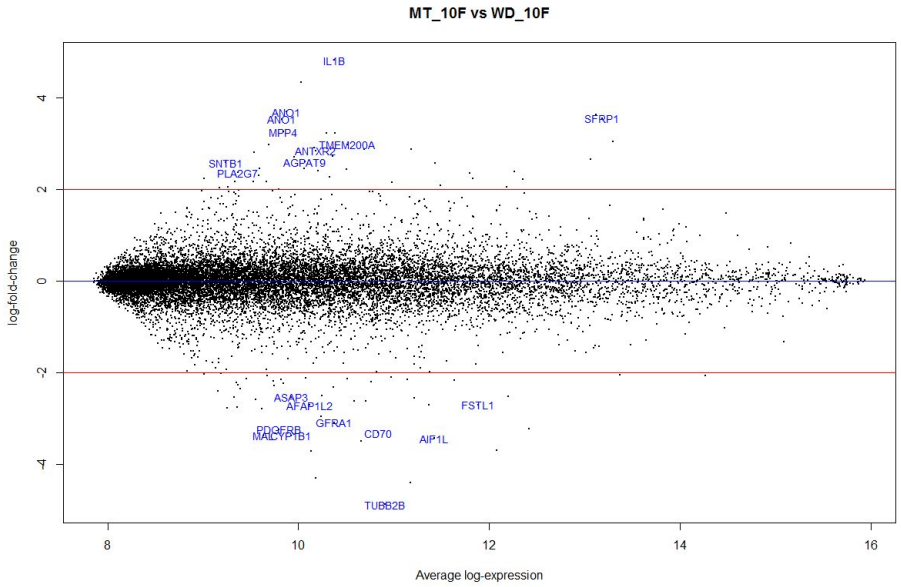

Figure 5. MA plot between BRAF wild type cells and BRAF mutant type cells, treated with growth factor. 2441 genes were up-regulated in BRAF mutant cells whereas 2724 genes are up-regulated in the wild type BRAF cells.

Table 1. Up-regulated DEGs and their gene ontology terms in Nthy/V600E mutant cells with growth factor treatment.

Genes	Full name	Log FC	BH *p*-value	Gene Ontology Terms
IL1B	interleukin 1, beta	4.826	6.89E-05	Activation of MAPK activity
ANO1	anoctamin 1, calcium activated chloride channel	4.339	< 0.001	Ion transmembrane transport, multicellular organismal development
SERPINE2	serpin peptidase inhibitor, clade E, member 2	3.634	< 0.001	Regulation of cell migration
SFRP1	secreted frizzled-related protein 1	3.553	< 0.001	Wnt receptor signaling pathway, regulation of peptidyl-tyrosine phosphorylation
MPP4	membrane protein, palmitoylated 4	3.260	< 0.001	Protein localization to synapse
KHDRBS3	KH domain containing, RNA binding, signal transduction associated 3	3.236	< 0.001	Regulation of transcription
TMEM200A	transmembrane protein 200A	2.988	< 0.001	Integral to membrane
IL24	interleukin 24	2.986	< 0.001	Regulation of cell proliferation
G0S2	G0/G1 switch 2	2.911	< 0.001	Regulation of apoptotic signaling pathway
ANTXR2	anthrax toxin receptor 2	2.847	< 0.001	Integral to membrane
FOXQ1	forkhead box Q1	2.820	< 0.001	Tissue development

DCLK1	doublecortin-like kinase 1	2.705	< 0.001	Protein kinase activity, phosphorylation
AGPAT9	1-acylglycerol-3-phosphate O-acyltransferase 9	2.601	< 0.001	Regulation of TOR signaling
SNTB1	syntrophin, beta 1	2.591	< 0.001	Protein binding, phospholipid binding
CALB2	calbindin 2	2.461	< 0.001	Calcium ion binding, cytoplasm, gap junction
PHLDA1	pleckstrin homology-like domain, family A, member 1	2.384	< 0.001	Protein binding, phospholipid binding, apoptotic process
PLA2G7	phospholipase A2, group VII	2.371	< 0.001	Regulation of inflammatory response
LAMB3	laminin, beta 3	2.360	< 0.001	Structural molecule activity, extracellular matrix organization
ITGA2	integrin, alpha 2	2.303	< 0.001	Cell-matrix adhesion, integrin-mediated signaling pathway
STC1	stanniocalcin 1	2.229	< 0.001	Cell surface receptor signaling pathway
NT5E	5'-nucleotidase, ecto (CD73)	2.156	< 0.001	DNA metabolic process, regulation of inflammatory response
TRIB1	tribbles pseudokinase 1	2.005	< 0.001	Protein kinase activity, regulation of MAP kinase activity

Table 2. Enriched gene ontologies in Nthy/V600E cells, treated with growth factor.

GO ID	Term	p-value	Significant Genes No.	Total Genes No.
GO:0008219	cell death	4.92E-10	62	1843
GO:0060560	developmental growth involved in morphogenesis	5.13E-10	17	166
GO:0016265	death	5.37E-10	62	1847
GO:0009653	anatomical structure morphogenesis	6.42E-10	74	2438
GO:0007155	cell adhesion	1.35E-09	50	1344
GO:0022610	biological adhesion	1.61E-09	50	1351
GO:0010941	regulation of cell death	2.12E-09	51	1406
GO:0012501	programmed cell death	4.18E-09	58	1755
GO:0030155	regulation of cell adhesion	6.33E-09	29	561
GO:0006915	apoptotic process	7.67E-09	57	1737
GO:0043067	regulation of programmed cell death	9.82E-09	48	1337
GO:0048585	negative regulation of response to stimulus	1.36E-08	45	1219
GO:0060429	epithelium development	1.38E-08	41	1049
GO:0042981	regulation of apoptotic process	2.26E-08	47	1328
GO:0008283	cell proliferation	3.27E-08	57	1809
GO:0042127	regulation of cell proliferation	3.90E-08	48	1397
GO:0040011	locomotion	4.96E-08	51	1546
GO:0009888	tissue development	4.97E-08	54	1687
GO:0009968	negative regulation of signal transduction	7.35E-08	38	986
GO:0032502	developmental process	7.58E-08	119	5301
GO:0016477	cell migration	8.57E-08	40	1077
GO:0048856	anatomical structure development	8.77E-08	109	4706

GO:0009605	response to external stimulus	1.72E-07	60	2047
GO:0048522	positive regulation of cellular process	1.81E-07	98	4116
GO:0048589	developmental growth	1.97E-07	22	404
GO:0006928	movement of cell or subcellular component	1.99E-07	52	1663
GO:0048583	regulation of response to stimulus	2.08E-07	83	3275
GO:0043065	positive regulation of apoptotic process	2.14E-07	26	547
GO:0007275	multicellular organismal development	2.16E-07	104	4483
GO:0044767	single-organism developmental process	2.40E-07	116	5217
GO:0043068	positive regulation of programmed cell death	2.55E-07	26	552
GO:0023057	negative regulation of signaling	2.58E-07	39	1079
GO:0048519	negative regulation of biological process	2.99E-07	98	4157
GO:0010648	negative regulation of cell communication	3.04E-07	39	1086
GO:0060602	branch elongation of an epithelium	3.49E-07	6	20
GO:0003401	axis elongation	3.84E-07	7	32
GO:0048468	cell development	4.70E-07	56	1906
GO:0042325	regulation of phosphorylation	4.80E-07	42	1240
GO:0008285	negative regulation of cell proliferation	4.89E-07	27	609
GO:0048513	organ development	4.94E-07	74	2845
GO:0010942	positive regulation of cell death	5.21E-07	26	573
GO:0048870	cell motility	5.86E-07	40	1159
GO:0051674	localization of cell	5.86E-07	40	1159
GO:0006468	protein phosphorylation	6.43E-07	46	1439
GO:0001763	morphogenesis of a branching structure	6.63E-07	15	210
GO:0048729	tissue morphogenesis	7.47E-07	26	584
GO:0019220	regulation of phosphate metabolic process	7.51E-07	46	1447
GO:0040007	growth	7.64E-07	33	866

GO:0022407	regulation of cell-cell adhesion	7.90E-07	19	336
GO:0035295	tube development	8.23E-07	26	587
GO:0051174	regulation of phosphorus metabolic process	9.65E-07	46	1460
GO:0009790	embryo development	1.18E-06	35	969
GO:1902532	negative regulation of intracellular signal transduction	1.18E-06	20	379
GO:0048731	system development	1.26E-06	92	3928
GO:0030154	cell differentiation	1.44E-06	83	3424
GO:0001932	regulation of protein phosphorylation	1.49E-06	36	1023
GO:0009966	regulation of signal transduction	1.52E-06	67	2549
GO:0002009	morphogenesis of an epithelium	1.63E-06	22	458
GO:0044763	single-organism cellular process	1.73E-06	203	11513
GO:0048518	positive regulation of biological process	1.80E-06	107	4851
GO:0061138	morphogenesis of a branching epithelium	1.89E-06	14	199
GO:0006469	negative regulation of protein kinase activity	2.12E-06	14	201
GO:0048869	cellular developmental process	2.49E-06	86	3640
GO:0048523	negative regulation of cellular process	2.64E-06	89	3818
GO:0051246	regulation of protein metabolic process	2.99E-06	58	2123
GO:0006935	chemotaxis	3.38E-06	27	674
GO:0042330	taxis	3.38E-06	27	674
GO:0072001	renal system development	3.47E-06	16	271
GO:0009887	organ morphogenesis	3.74E-06	32	888
GO:0016049	cell growth	3.79E-06	20	409
GO:0040012	regulation of locomotion	4.16E-06	26	641
GO:0001655	urogenital system development	4.62E-06	17	310
GO:0033673	negative regulation of kinase activity	4.67E-06	14	215
GO:0048598	embryonic morphogenesis	5.17E-06	24	569

Table 3. Enriched pathways by up-regulated DEGs in Nthy/V600E cells with growth factor treatment. Analysis was performed by DAVID.

Term	Count	%	p-value	Total genes
hsa03010:Ribosome	21	0.207	2.33E-08	87
hsa04210:Apoptosis	14	0.138	7.56E-04	87
hsa00600:Sphingolipid metabolism	8	0.079	0.005	39
hsa05222:Small cell lung cancer	11	0.108	0.015	84
hsa05014:Amyotrophic lateral sclerosis (ALS)	8	0.079	0.024	53
hsa04940:Type I diabetes mellitus	7	0.069	0.025	42
hsa05200:Pathways in cancer	27	0.266	0.032	328
hsa05130:Pathogenic Escherichia coli infection	8	0.079	0.035	57
hsa05210:Colorectal cancer	10	0.098	0.038	84
hsa00750:Vitamin B6 metabolism	3	0.030	0.038	6
hsa04110:Cell cycle	13	0.128	0.039	125
hsa04640:Hematopoietic cell lineage	10	0.098	0.043	86
hsa04115:p53 signaling pathway	8	0.079	0.075	68

Discussion

Characteristics of our Nthy/V600E cells were as follows: (1) Shape change into spindle type, (2) Overexpression of p-ERK and MAPK related genes, (3) Increased anchorage-independent growth and invasion potential, (4) Enrichment of cancer related pathways.

Cell shape change in Nthy/V600E may be derived from the epithelial-mesenchymal transition (EMT) induced by BRAF mutation. Previous study had reported that thyroid cancer cells were differed from epithelial shape of the wild type thyroid cells, and appeared as a spindle-shaped phenotype in BrafV600E mice (14). The hallmark of EMT is the down-regulation of E-cadherin and the up-regulation of vimentin expression and a significant loss of E-cadherin gene expression and an increase in vimentin gene expression was seen in the BRAFV600E thyroid tumors compared to normal thyroid (14). In rat thyroid PCCL3 cell line, over-expression of BRAFV600E promoted EMT and cellular invasion through the operation of an autocrine transforming growth factor (TGF)β loop (1). In accordance with previous reports, genes known to be associated with EMT, i.e. vimentin, was highly expressed in Nthy/V600E cells, compared to Nthy/WT cells in our microarray experiments (data not shown).

Oncogenic BRAF protein is continuously phospharylated and hence activates ERK signaling pathway. The mechanism of phosphorylation of oncogenic BRAF protein has been found through the study of Wan et al. in 2004. Normal BRAF protein is maintained in the condition which ATP combination domain is attached to phosphorylation domain and prohibits

phosphorylation. In the mutant BRAF, the combination is scattered away and always activates to be phosphorylation (15). PLX-4032 is a commercially available BRAFV600E selective inhibitor. In cells harboring BRAFV600E mutation, PLX-4032 inhibits the MAP kinase signaling effectively and suppresses ERK phosphorylation by selective binding to the mutant protein. In tumor xenograft models of BRAFV600E expressing melanoma, PLX-4032 suppresses tumor growth and improves survival of animal in a dose dependent manner (16,17). Likewise, PLX-4032 inhibited anchorage independent growth of Nthy/V600E cells in our study (Figure 3). In a study using rat PCCL3 clonal cell lines with doxycycline-inducible expression of BRAFV600E, BRAFV600E protein expression and ERK phosphorylation was doxycycline dose-dependent (6,18).

In another study using PCCL3 cells with doxycycline-inducible expression of BRAFV600E, treatment of doxycycline induced Matrigel invasion (19). In a study using human PTC-derived cell lines KAT5 and KAT10, both harboring a heterozygous BRAFV600E mutation, stable knockdown of BRAF gene using BRAF small interference RNA (siRNA) suppress anchorage-independent colony formation in soft agar (20). Our human thyrocyte cell-based results are in accordance with with previous reports using rat thyrocyte cell lines or human thyroid carcinoma cell lines.

In microarray analysis, enriched gene ontologies supported our functional experiment results.. DEGs that were up-regulated in Nthy/V600E cells are associated with cancer related pathways. These results reveal that Nthy/V600E cells are more closely related to carcinomas than Nthy/Vector or Nthy/WT cells. Specifically, top three up-regulated genes in Nthy/V600E

cells are already described to be associated with carcinomas.

IL-1 is a principal components of the interleukin family (21). In in vitro analysis using melanocytes and melanoma cell lines, expression of BRAFV600E enhanced the transcription of IL-1α and IL-1β and when BRAFV600E was inhibited, transcription of human IL-1α and IL-1β was reduced (22,23). IL-1β also known to be disturb epithelial tightness of human thyrocytes by altering expression and localization of junction proteins, probably promoting tumor growth (24). IL-1β induces the activation of cAMP responsive element-binding protein (CREB) through ERK1/2 signaling and this mechanism was associated with poor prognosis in gastric carcinoma, non-small cell lung cancer and breast cancer patients in previous reports (25-27).

ANO1 gene transcribes "ANO1 (Also known as transmembrane member 16A (TMEM16A)) which act as voltage sensitive calcium activated chloride channel (28). In a study in head and neck squamous cell carcinoma, ANO1 overexpression was associated with anchorage-independent growth in vitro and tumor growth in vivo, whereas loss of ANO1 resulted in inhibition of tumor growth. ANO1-induced cell proliferation and tumor growth were accompanied by an increase in ERK 1/2 activation and cyclin D1 induction (29). In lung cancer and colorectal cancer study, ANO1 over-expression was related with tumor growth and invasion (30,31).

SERPINE2 gene encodes a member of serpine protein family proteins that inhibit serine proteases. In a study using human colorectal cell lines, BRAFV600E mutation can increase SERPINE2 mRNA and protein expression level (32). In a pancreatic cancer study using nude mouse xenografts, SERPINE2 overexpression raised the potential of invasion

through the extracellular matrix. Also, cancer cells in SERPINE2-expressing tumors show spindle-shaped morphology and expressed the mesenchymal intermediate filament marker vimentin, concordance with our experimental results (33).

Our Nthy/V600E cells show spindle-shaped morphology, anchorage-independent cellular growth pattern, increased invasive potential, and enhanced ERK phosphorylation. These cellular behaviors of Nthy/V600E cells are supported by enriched gene ontologies (Cell adhesion, migration, prolifetaion, etc.) in microarray analysis. TOP-3 overexpressed genes also associated with ERK1/2, MAPK cascade and cancer related pathway. Nthy/BRAF cells may be a good source for basic research to evaluate the effect of BRAFV600E mutation in normal thyroid cells.

In conclusion, we obtained a new cell line model to study carcinogenic mechanism of BRAFV600E mutation. Functional experiments and microarray data revealed that Nthy/V600E cell have enhanced growth potential, invasion ability and increased expression of MAPK pathway. Our Nthy/WT and Nthy/BRAF cell lines, with its correlation with human BRAFV600E PTCs, may be used as a good source for basic experiments to reveal molecular characteristics of thyroid cancer, according to BRAF mutation.

References

1. Nucera C, Goldfarb M, Hodin R, Parangi S. Role of B-Raf(V600E) in differentiated thyroid cancer and preclinical validation of compounds against B-Raf(V600E). Biochimica et biophysica acta. 2009;1795(2):152-161.

2. Garnett MJ, Marais R. Guilty as charged: B-RAF is a human oncogene. Cancer cell. 2004;6(4):313-319.

3. Carta C, Moretti S, Passeri L, Barbi F, Avenia N, Cavaliere A, Monacelli M, Macchiarulo A, Santeusanio F, Tartaglia M, Puxeddu E. Genotyping of an Italian papillary thyroid carcinoma cohort revealed high prevalence of BRAF mutations, absence of RAS mutations and allowed the detection of a new mutation of BRAF oncoprotein (BRAF(V599lns)). Clinical endocrinology. 2006;64(1):105-109.

4. Kim TY, Kim WB, Song JY, Rhee YS, Gong G, Cho YM, Kim SY, Kim SC, Hong SJ, Shong YK. The BRAF mutation is not associated with poor prognostic factors in Korean patients with conventional papillary thyroid microcarcinoma. Clinical endocrinology. 2005;63(5):588-593.

5. Ahn D, Park JS, Sohn JH, Kim JH, Park S-K, Seo AN, Park JY. BRAFV600E mutation does not serve as a prognostic factor in Korean patients with papillary thyroid carcinoma. Auris Nasus Larynx. 2012;39(2):198-203.

6. Mitsutake N, Knauf JA, Mitsutake S, Mesa C, Jr., Zhang L, Fagin JA. Conditional BRAFV600E expression induces DNA synthesis, apoptosis,

dedifferentiation, and chromosomal instability in thyroid PCCL3 cells. Cancer research. 2005;65(6):2465-2473.

7. Ball DW, Jin N, Rosen DM, Dackiw A, Sidransky D, Xing M, Nelkin BD. Selective growth inhibition in BRAF mutant thyroid cancer by the mitogen-activated protein kinase kinase 1/2 inhibitor AZD6244. The Journal of clinical endocrinology and metabolism. 2007;92(12):4712-4718.

8. Lemoine NR, Mayall ES, Jones T, Sheer D, McDermid S, Kendall-Taylor P, Wynford-Thomas D. Characterisation of human thyroid epithelial cells immortalised in vitro by simian virus 40 DNA transfection. British journal of cancer. 1989;60(6):897-903.

9. Eisenberg MC, Kim Y, Li R, Ackerman WE, Kniss DA, Friedman A. Mechanistic modeling of the effects of myoferlin on tumor cell invasion. Proceedings of the National Academy of Sciences of the United States of America. 2011;108(50):20078-20083.

10. Ritchie ME, Phipson B, Wu D, Hu Y, Law CW, Shi W, Smyth GK. limma powers differential expression analyses for RNA-sequencing and microarray studies. Nucleic acids research. 2015;43(7):e47.

11. Donath A, Kaser H, Roos B, Ziegler W, Oetliker O, Colombo JP, Bettex M. [Familial pheochromocytoma. Discussion of its malignancy and hereditary character: apropos of a case in a child with peculiar secretion]. Helvetica paediatrica acta. 1965;20(1):1-18.

12. Falcon S, Gentleman R. Using GOstats to test gene lists for GO term association. Bioinformatics (Oxford, England). 2007;23(2):257-258.

13. Team RC. R: A language and environment for statistical computing. R Foundation for Statistical Computing. 2015.

14. Ma R, Bonnefond S, Morshed SA, Latif R, Davies TF. Stemness is Derived from Thyroid Cancer Cells. Frontiers in endocrinology. 2014;5:114.

15. Wan PT, Garnett MJ, Roe SM, Lee S, Niculescu-Duvaz D, Good VM, Jones CM, Marshall CJ, Springer CJ, Barford D, Marais R. Mechanism of activation of the RAF-ERK signaling pathway by oncogenic mutations of B-RAF. Cell. 2004;116(6):855-867.

16. Xing J, Liu R, Xing M, Trink B. The BRAFT1799A mutation confers sensitivity of thyroid cancer cells to the BRAFV600E inhibitor PLX4032 (RG7204). Biochemical and biophysical research communications. 2011;404(4):958-962.

17. Yang H, Higgins B, Kolinsky K, Packman K, Go Z, Iyer R, Kolis S, Zhao S, Lee R, Grippo JF, Schostack K, Simcox ME, Heimbrook D, Bollag G, Su F. RG7204 (PLX4032), a selective BRAFV600E inhibitor, displays potent antitumor activity in preclinical melanoma models. Cancer research. 2010;70(13):5518-5527.

18. Melillo RM, Castellone MD, Guarino V, De Falco V, Cirafici AM, Salvatore G, Caiazzo F, Basolo F, Giannini R, Kruhoffer M, Orntoft T, Fusco A, Santoro M. The RET/PTC-RAS-BRAF linear signaling cascade mediates the motile and mitogenic phenotype of thyroid cancer cells. The Journal of clinical investigation. 2005;115(4):1068-1081.

19. Mesa C, Jr., Mirza M, Mitsutake N, Sartor M, Medvedovic M, Tomlinson C, Knauf JA, Weber GF, Fagin JA. Conditional activation of RET/PTC3 and BRAFV600E in thyroid cells is associated with gene expression profiles that predict a preferential role of BRAF in extracellular matrix remodeling. Cancer research. 2006;66(13):6521-6529.

20. Liu D, Liu Z, Condouris S, Xing M. BRAF V600E maintains proliferation, transformation, and tumorigenicity of BRAF-mutant papillary thyroid cancer cells. The Journal of clinical endocrinology and metabolism. 2007;92(6):2264-2271.

21. Dinarello CA. The interleukin-1 family: 10 years of discovery. FASEB journal : official publication of the Federation of American Societies for Experimental Biology. 1994;8(15):1314-1325.

22. Khalili JS, Liu S, Rodriguez-Cruz TG, Whittington M, Wardell S, Liu C, Zhang M, Cooper ZA, Frederick DT, Li Y, Zhang M, Joseph RW, Bernatchez C, Ekmekcioglu S, Grimm E, Radvanyi LG, Davis RE, Davies MA, Wargo JA, Hwu P, Lizee G. Oncogenic BRAF(V600E) promotes stromal cell-mediated immunosuppression via induction of interleukin-1 in melanoma. Clinical cancer research : an official journal of the American Association for Cancer Research. 2012;18(19):5329-5340.

23. Khalili JS, Hwu P, Lizee G. Forging a link between oncogenic signaling and immunosuppression in melanoma. Oncoimmunology. 2013;2(2):e22745.

24. Rebuffat SA, Kammoun-Krichen M, Charfeddine I, Ayadi H, Bougacha-Elleuch N, Peraldi-Roux S. IL-1beta and TSH disturb thyroid epithelium integrity in autoimmune thyroid diseases. Immunobiology. 2013;218(3):285-291.

25. Resende C, Regalo G, Duraes C, Pinto MT, Wen X, Figueiredo C, Carneiro F, Machado JC. Interleukin-1B signalling leads to increased survival of gastric carcinoma cells through a CREB-C/EBPbeta-associated mechanism.

Gastric cancer : official journal of the International Gastric Cancer Association and the Japanese Gastric Cancer Association. 2016;19(1):74-84.

26. Sun H, Chung WC, Ryu SH, Ju Z, Tran HT, Kim E, Kurie JM, Koo JS. Cyclic AMP-responsive element binding protein- and nuclear factor-kappaB-regulated CXC chemokine gene expression in lung carcinogenesis. Cancer prevention research (Philadelphia, Pa). 2008;1(5):316-328.

27. Chhabra A, Fernando H, Watkins G, Mansel RE, Jiang WG. Expression of transcription factor CREB1 in human breast cancer and its correlation with prognosis. Oncology reports. 2007;18(4):953-958.

28. Yang YD, Cho H, Koo JY, Tak MH, Cho Y, Shim WS, Park SP, Lee J, Lee B, Kim BM, Raouf R, Shin YK, Oh U. TMEM16A confers receptor-activated calcium-dependent chloride conductance. Nature. 2008;455(7217):1210-1215.

29. Duvvuri U, Shiwarski DJ, Xiao D, Bertrand C, Huang X, Edinger RS, Rock JR, Harfe BD, Henson BJ, Kunzelmann K, Schreiber R, Seethala RS, Egloff AM, Chen X, Lui VW, Grandis JR, Gollin SM. TMEM16A induces MAPK and contributes directly to tumorigenesis and cancer progression. Cancer research. 2012;72(13):3270-3281.

30. Jia L, Liu W, Guan L, Lu M, Wang K. Inhibition of Calcium-Activated Chloride Channel ANO1/TMEM16A Suppresses Tumor Growth and Invasion in Human Lung Cancer. PloS one. 2015;10(8):e0136584.

31. Sui Y, Sun M, Wu F, Yang L, Di W, Zhang G, Zhong L, Ma Z, Zheng J, Fang X, Ma T. Inhibition of TMEM16A expression suppresses growth and invasion in human colorectal cancer cells. PloS one. 2014;9(12):e115443.

32. Bergeron S, Lemieux E, Durand V, Cagnol S, Carrier JC, Lussier JG, Boucher MJ, Rivard N. The serine protease inhibitor serpinE2 is a novel target of ERK signaling involved in human colorectal tumorigenesis. Molecular cancer. 2010;9:271.

33. Buchholz M, Biebl A, Neesse A, Wagner M, Iwamura T, Leder G, Adler G, Gress TM. SERPINE2 (protease nexin I) promotes extracellular matrix production and local invasion of pancreatic tumors in vivo. Cancer research. 2003;63(16):4945-4951.

요약 (국문초록)

서론: $BRAF^{V600E}$ 돌연변이는 갑상선 유두암(Papillary thyroid carcinoma, PTC)에서 가장 흔한 변이로 갑상선암에서 종양 발생의 초기에서부터 작용하는 것으로 여겨진다. 따라서 $BRAF^{V600E}$ 돌연변이에 의해 발생하는 2차적인 유전자 발현의 변화가 갑상선암의 예후 및 성장에 중요한 역할을 하리라 생각되며 이에 대한 연구가 필요하다.

방법: 갑상선암에서 $BRAF^{V600E}$ 돌연변이에 의해 발생하는 타 유전자 변이에 대해 연구하기 위해, 본 연구에서는 정상 갑상선 세포주(Nthy-ori 3-1)에 유전자 형질도입을 통하여 정상 BRAF 유전자를 발현하는 갑상선 세포 모델 (Nthy/WT)과 $BRAF^{V600E}$ 돌연변이를 발현하는 갑상선 세포 모델 (Nthy/V600E)을 제작하였다. DNA 염기서열분석, 유세포 분석(flow cytometry), 웨스턴 블럿(western blot) 을 통하여 형질도입이 잘 이루어졌는지 확인하고 $BRAF^{V600E}$ 돌연변이로 인한 세포의 기능적인 변화를 군집 형성 능력 평가(Colony forming assay)와 침윤성 평가 (Invasion assay)를 통해 관찰하였다. 최종적으로 유전자미세배열(Microarray)을 통해 Nthy/WT와 Nthy/V600E의 유전자 발현 차이를 평가하고 $BRAF^{V600E}$ 돌연변이를 가지는 세포 모델에서 유의하게 발현이 증가하는 유전자를 선별한다.

결과: 정상 갑상선 세포주(Nthy-ori 3-1)에 BRAF 유전자를 안정적으로 형질도입 하였고 Nthy/WT와 다르게 Nthy/V600E에서는 $BRAF^{V600E}$의 특징인 인산화-ERK의 발현(phophorylated ERK levels)이 증가되었다. 기능적인 측면을 평가해 본 결과 Nthy/V600E 세포에서 부착 비의존성 성장(Anchorage-independent grow)과 침윤성이 유의하게 증가하였다. 유전자 미세배열 분석 결과, 2441개의 유전자가 Nthy/WT에 비해서 Nthy/V600E에서 발현이 증가하였고 IL1B, ANO1, SERPINE2 유

전자가 가장 큰 차이를 보였다. Nthy/V600E에서 발현이 증가한 유전자들은(Up-regulated genes) 유전자 온톨로지(Gene Ontology) 분석에서 세포 접착(cell adhesion), 세포 이동(migration), 운동성(motility), ERK와 MAPK(Mitogen-activated protein kinases) cascade와 관련이 있는 것으로 나타났다. 경로 분석(pathway analysis)에서 또한 암과 관련된 경로가 높게 나타났다.

결론: 본 연구에서는 인간 갑상선 유두암에서 $BRAF^{V600E}$ 돌연변이의 발암 기전을 연구할 수 있는 새로운 실험 모델인 Nthy/WT 와 Nthy/V600E 세포 모델을 확보하였고 BRAF 돌연변이에 수반되는 유전자 발현 양상의 변화를 밝혔다.

주요어: 갑상선, Nthy-ori 3-1 세포주, BRAF ^{V600E} 돌연변이, 형질도입, 유전자미세배열

학 번: 2014-25079